

Article

Comparative Study on Convection and Wall Characteristics of Al₂O₃—Water Nanofluid Flow inside a Miniature Tube

Aminhossein Jahanbin

DIN—Department of Industrial Engineering, University of Bologna, Viale Risorgimento 2, 40136 Bologna, Italy
E-mail: aminhossein.jahanbin@unibo.it

Abstract. Forced convective heat transfer and wall characteristics of nanofluid flow containing Al₂O₃ nanoparticles and water inside a miniature tube is studied numerically by means of computational fluid dynamic (CFD) code. Problem is solved by employing finite volume approach using both single-phase (homogeneous) and dispersion models. In both models, constant and temperature-dependent thermophysical properties are used and results are compared to available experimental and theoretical literatures.

It can be seen as the Reynolds number increases, the Nusselt number improves, too. However, it is accompanied by higher wall shear stress. Moreover, in the case of temperature-dependent properties, lower values for shear stress were obtained. In comparison with experimental data and available theoretical correlations, dispersion model in both temperature-dependent and constant properties shows a desirable compatibility. On the other hand, single-phase model in constant thermophysical properties underestimates the amount of convective heat transfer. Furthermore, it can be observed at wall, by increasing the particles volume concentration, not only wall temperature decreases also, rate of thermal enhancement decreases slightly.

Keywords: Convective heat transfer, nanofluids, computational fluid dynamics, shear stress, temperature-dependent properties, dispersion model.

ENGINEERING JOURNAL Volume 20 Issue 3

Received 23 September 2015

Accepted 5 January 2016

Published 19 August 2016

Online at <http://www.engj.org/>

DOI:10.4186/ej.2016.20.3.169

1. Introduction

Many industrial processes for energy conversion and transmission may be related to the fluid and its flow. Processes that comprise a wide range of temperatures, heat fluxes and various pressures under different flow regimes and they will often benefit from reducing thermal resistance that will be led to the optimization of energy and accordingly reduction of costs.

Low thermal conductivity of common fluids in industry is the first restriction to develop optimized heat transfer, which it has been evolved more severely by appearance of micro-scale systems (MEMS), where cooling operation is to be one of the most rudimentary requirements. Producing particles in nano-scales along with the nanotechnology, ended up to appearance of a new category of fluids calling as "Nanofluids". Nowadays, fast growth of researches on the nanoparticles and nanofluids' thermal properties shows the importance of this Generation of fluids. The various reviews regarding nanofluids have shown that they have desired thermal properties such as thermal conductivity, heat transfer coefficient and high critical heat flux compared to classic working fluids such as water or ethylene glycol. These key features together with remarkable stability and having no portion in previous rheological problems, unlocks the door on their use in an extensive range of engineering applications such as engine cooling, microelectronics devices and medical applications including treatment of cancer.

Researches on the nanofluids' behaviors have almost commenced since the beginning of the twenty first century and annual publication of nanofluids has remarkably increased from 1999 to 2005 that has grown to more than 70% [1]. In the previous decade, many studies have carried out about heat transfer of nanofluids in both experimental and numerical methods for different type and size of particles in various geometries. Although the thermal conductivity of nanofluids is considered as an encouraging feature for their use, a significant role is contributed to convection as it is a criterion of applicability and shows superiority of their heat transfer in comparison with other fluids. Wen and Ding [2] did an experimental study on nanofluids convective heat transfer in entrance region of a channel containing γ - Al_2O_3 particles and water as a host fluid in a laminar flow. They found out that convective heat transfer of nanofluid depends on more factors than only thermal conductivity such as particles motion and the reduction of boundary layer thickness.

Heris et al. [3–5] investigated convective heat transfer of nanofluids containing copper (Cu), copper oxide (CuO) and aluminum oxide (Al_2O_3) nanoparticles in water based fluid numerically. They study heat transfer coefficient of nanofluids through miniature tubes with different cross-section geometries. They also, validated their numerical results with their experimental data [6], which showed appropriate agreement. The results showed that by using Al_2O_3 particles heat transfer rate increased by 40% while increasing the thermal conductivity coefficient was less than 15%.

Numerical Investigation of forced convective heat transfer of nanofluid in both laminar and turbulent flow inside a circular tube, carried out by Bianco et al. [7, 8]. The results showed the heat transfer always improves, as Reynolds number increases, but it is accompanied by an increase of shear stress, too. Also, both single-phase and two-phase models were considered in their study. However, single-phase model results underestimated the heat transfer coefficient compared with two-phase model.

Forced convective heat transfer of a nanofluid consisting of water and Al_2O_3 in horizontal tube studied numerically by Lotfi et al. [9]. Different models of two-phase flow considered for nanofluid and also, the effect of particle concentration on convection was taken into account. The comparison between calculated results and experimental values showed that the mixture model is more precise.

Moreover, Jahanbin et al. [10] carried out an investigation on forced convective heat transfer of nanofluid in laminar flow regime inside a tube with circular cross-section. Nanofluid contained CuO nanoparticles with 50 nanometer diameter in water base fluid. It was shown in the presence of nanoparticles the heat transfer coefficient increases to some considerable extent and the heat transfer enhancement strongly depends on the volume concentration of nanoparticles and Peclet number.

It can be said that the next stage of researches on nanofluids convective heat transfer will be significantly focused on the physical associated mechanisms and also, methodology. The scope of this study is to analyze the convection and wall characteristics of Al_2O_3 -water nanofluid flow inside a miniature channel. The finite volume method was employed to solve the problem by utilizing two different models in both constant and temperature-dependent thermophysical properties and to compare the results with various experimental data and theoretical correlations. Moreover, temperature and shear stress at wall in

Nomenclature

c_p	heat capacity of air ($\text{J kg}^{-1} \text{K}^{-1}$)		
D	tube diameter (m)		
d	thermal diffusivity due to dispersion ($\text{m}^2 \text{s}^{-1}$)		
h	heat transfer coefficient ($\text{W m}^{-2} \text{K}^{-1}$)		
H	half of the channel height (m)		
k	thermal conductivity ($\text{W m}^{-1} \text{K}^{-1}$)		
L	tube length (m)		
Nu	Nusselt number		
p	pressure (Pa)		
Pe	Peclet number		
q	heat flux (W m^{-2})		
r	radial variable		
Re	Reynolds number		
T	temperature (K)		
u	velocity magnitude (m s^{-1})		
\vec{u}	velocity vector (m s^{-1})		
x	axial variable		
		<i>Greek symbols</i>	
		α	thermal diffusivity ($\text{m}^2 \text{s}^{-1}$)
		μ	dynamic viscosity ($\text{kg m}^{-1} \text{s}^{-1}$)
		φ	particle volume concentration
		ρ	fluid density (kg m^{-3})
		τ	shear stress (Pa)
			<i>Subscripts / Superscripts</i>
		av	average value
		bf	refers to base fluid property
		d	refers to dispersion model
		eff	effective value
		m	mean value
		nf	refers to nanofluid property
		p	refers to particle property
		r	radial direction
		x	axial direction
		0	refers to initial value

presence of nanoparticles were studied and the effect of particle concentration on heat transfer was investigated. The purpose is to add a further contribution to the field of convective heat transfer of nanofluids where it seems to be still open-ended despite vast amount of publications.

2. Mathematical Modeling

2.1. Geometrical Configuration and Boundary Condition

Geometry and boundary condition of the problem under consideration are illustrated in Fig. 1. The tube has a circular cross-section and length of L ($L=1.0$ m) and diameter of D ($D=10$ mm) and is made of copper (Cu). The ratio of length to diameter is considered as $L/D=100$, in order to obtain fully developed profiles.

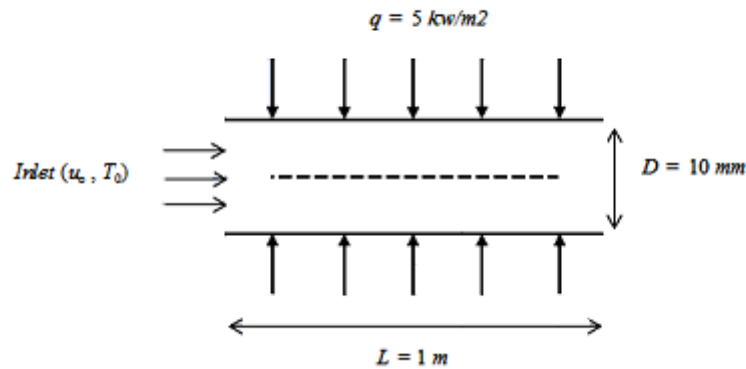


Fig.1. Schematic of the geometry and boundary condition under consideration.

At the inlet laminar steady-state uniform flow with axial velocity of u_0 and temperature of T_0 enters to the tube at atmospheric pressure. The initial temperature T_0 is equal to 293 K. Also, fluid flow and thermal

field were assumed to be 2D symmetrical and in order to save computational time half of the tube was considered in numerical simulation. At the wall, uniform constant heat flux boundary condition prevails and non-slip condition is imposed.

2.2. Thermophysical Properties

Since determination of thermophysical properties affects directly the results, most appropriate theoretical and experimental correlations were employed in this study. Both correlations for constant and temperature-dependent properties are introduced. By assuming that nanoparticles are well dispersed within the host fluid, effective properties for constant properties are [11, 12]:

$$\rho_{nf} = (1 - \varphi)\rho_{bf} + \varphi\rho_p \quad (1)$$

$$c_{p_{nf}} = (1 - \varphi)c_{p_{bf}} + \varphi c_{p_p} \quad (2)$$

$$\mu_r = \frac{\mu_{nf}}{\mu_{bf}} = 123\varphi^2 + 7.3\varphi + 1 \quad (3)$$

$$k_r = \frac{k_{nf}}{k_{bf}} = 4.97\varphi^2 + 2.72\varphi + 1 \quad (4)$$

In the case of temperature-dependent properties, for computing viscosity and thermal conductivity of base fluid, the models based on the Bianco et al. [7] correlations were used:

$$\mu_{bf} = -6.37 \times 10^{-4} T + 1.80 \times 10^{-6} T^2 - 1.73 \times 10^{-9} T^3 + 7.57 \times 10^{-2} \quad (5)$$

$$k_{bf} = 9.71 \times 10^{-3} T - 1.31 \times 10^{-5} T^2 - 1.13 \quad (6)$$

Palm et al. [13] by curve-fitting of Putra et al. [14]'s experimental data, proposed the following correlations for Al₂O₃-water nanofluid in two different particle concentrations:

for $\varphi = 1\%$:

$$\mu_{nf} = 2.912 \times 10^{-7} T^2 - 2.0 \times 10^{-4} T + 3.4 \times 10^{-2} \quad (7)$$

$$k_{nf} = 0.003352T - 0.3708 \quad (8)$$

for $\varphi = 4\%$:

$$\mu_{nf} = 3.475 \times 10^{-7} T^2 - 2.353 \times 10^{-4} T + 4.051 \times 10^{-2} \quad (9)$$

$$k_{nf} = 0.004961T - 0.8078 \quad (10)$$

2.3. Governing Equations

Single-phase and dispersion models were employed for modeling the nanofluid problem in both constant and temperature-dependent thermophysical properties. For both methods corresponding equations were introduced separately.

2.3.1. Single-phase model

In single-phase or homogeneous model it is considered there is no slip between nanoparticles and base fluid. Under this assumption, both base fluid and solid nanoparticles are in thermal equilibrium, so, in the presence of nanoparticles, the flow and energy equations are not affected. In this case, the only thing that should be taken into account is using the effective properties instead of pure fluid's properties. Mass conservation, momentum and energy equations are introduced as following, respectively

$$\text{div}(\rho\vec{u}) = 0 \quad (11)$$

$$\operatorname{div}(\rho \bar{u} \bar{u}) = -\operatorname{grad} p + \nabla \cdot (\mu \nabla^2 \bar{u}) \quad (12)$$

$$\operatorname{div}(\rho \bar{u} c_p T) = \operatorname{div}(k \operatorname{grad} T) \quad (13)$$

2.3.2. Dispersion model

Due to the effects of various factors such as gravity, Brownian diffusion, friction between the fluid and nanoparticles, nanofluids in fact, are a two-phase suspension in nature. Under this hypothesis, it can be said that dispersion may co-exist in main flow and motion slip is not equal to zero. Xuan and Roetzel [15] formulated this effect for the nanofluids under assumption that irregular and random movement of the particles in base fluid increases the energy exchange rate, i.e, thermal dispersion takes place in the flow and it flattens the temperature distribution and makes the temperature gradient between the wall and fluid steeper, which enhances the heat transfer rate. They postulated due to perturbation, irregular and random movements of ultrafine particles, another terms of temperature T' and velocity \bar{u}' can be added in nanofluids' energy equation. Thus, it reads:

$$T = \langle T \rangle^{bf} + T' \quad (14)$$

$$\bar{u} = \langle \bar{u} \rangle^{bf} + \bar{u}' \quad (15)$$

where

$$\langle T \rangle^{bf} = \frac{1}{V_f} \int_V T \, dV \quad (16)$$

$$\langle \bar{u} \rangle^{bf} = \frac{1}{V_f} \int_V \bar{u} \, dV \quad (17)$$

$$\frac{1}{V_f} \int_V T' \, dV = 0 \quad (18)$$

By considering that boundary layer between the fluid and nanoparticles is negligible, energy equation (Eq. (13)) can be written as:

$$(\rho c_p)_{nf} \left[\langle \bar{u} \rangle^{bf} \cdot \nabla \langle T \rangle^{bf} \right] = \nabla \cdot (k_{nf} \nabla \langle T \rangle^{bf}) - (\rho c_p)_{nf} \nabla \cdot \langle \bar{u}' T' \rangle^{bf} \quad (19)$$

Also, the heat flux corresponding to thermal dispersion in fluid flow can be expressed as:

$$q_d = (\rho c_p)_{nf} \langle \bar{u}' T' \rangle^{bf} = -\mathbf{k}_d \cdot \nabla \langle T \rangle^{bf} \quad (20)$$

where \mathbf{k}_d is the tensor of thermal conductivity due to dispersion. Now Eq. (13) can be rewritten as:

$$\langle \bar{u} \rangle^{bf} \cdot \nabla \langle T \rangle^{bf} = \nabla \cdot \left[\left(\alpha_{nf} \mathbf{I} + \frac{\mathbf{k}_d}{(\rho c_p)_{nf}} \right) \cdot \nabla \langle T \rangle^{bf} \right] \quad (21)$$

where α is thermal diffusivity and \mathbf{I} is the identity tensor. Effective thermal conductivity of nanofluid by considering both molecular and dispersion effects may take the following form:

$$k_{eff} = k_{nf} + k_d \quad (22)$$

So far there is neither certain theoretical nor experimental correlation to calculate thermal conductivity tensor due to dispersion. In 1954, Sir Geoffrey Taylor [16] for thermal diffusion coefficient of water-salt solution proposed the following correlation, verified later by Aris [17]:

$$\frac{d_d}{\alpha_{bf}} = \frac{(r^2 u_m^2)}{48 \alpha_{bf}^2} = \frac{1}{48} Pe^2 \quad (23)$$

However, this result was specifically for salt and water solution and it does not seem to be satisfying for nanofluids. Khaled and Vafai [18] in their literature investigated heat transfer enhancement through control of dispersion effects. They developed the following form for dispersed thermal conductivity of nanofluid by using porous media theory:

$$k_d = C^* (\rho c_p)_{nf} \varphi H u_m \quad (24)$$

where H is the half of channel and u_m is average bulk velocity and also, C^* is an unknown constant. They proposed in their literature range of 0-0.4 for the unknown constant C^* . By considering the mentioned range and comparing the results with experimental data, in the present study C^* was set equal to 0.01.

In order to analyze the convection, heat transfer coefficient and Nusselt number are needed to be obtained. Local and average heat transfer coefficient and Nusselt number for bulk flow are defined as:

$$h_x = \frac{q}{[T_w(x) - T_f(x)]} \quad (25)$$

$$Nu_x = \frac{h_x \cdot D}{k_0} \quad (26)$$

$$h_{av} = \frac{1}{L} \int_0^L h(x) dx \quad (27)$$

$$Nu_{av} = \frac{h_{av} \cdot D}{k_0} \quad (28)$$

2.4. CFD Modeling and Code Validation

The governing equations were solved by using finite volume approach. The computational fluid dynamic code was employed to solve a set of the algebraic discretized equations in spatial integration process. For discretization of energy and momentum equations, Second Order Upwind Scheme [19] was employed and Green-Gauss cell based method was used for derivatives estimation. Moreover, SIMPLE-C algorithm (Semi Implicit Method for Pressure Linked Equation – Consistent) was considered for coupling the pressure field-velocity. Also, in order to accelerate the convergence, under-relaxation factors for momentum and energy equations were used. The residuals resulting from integration of the algebraic discretized equations over the control volume were considered as convergence indicators. The convergence was assumed to be reached when the residuals of continuity, momentum and energy were less than 10^{-3} , 10^{-3} , and 10^{-7} , respectively.

In order to obtain precise results, different non-uniform grids were checked. Table 1 shows the grid independence of the CFD problem. The 700×200 non-uniform grid was chosen for meshing the physical domain since showed negligible discrepancy in Nusselt number. Also, meshing of the physical domain was subjected to highly concentrated grid points in the vicinity of wall, inlet and outlet of the tube where higher velocity and temperature gradients exist.

Table 1. Grid independence of computational results (base fluid for $Re=750$).

Grid cells in x-dir	Grid cells in r-dir	Nu_{av}
540	42	6.607
700	20	6.628
780	32	6.606

Numerical code has been validated by means of well-known Shah's correlation, reported in [20]. Fig. 2 shows the desirable accuracy of the grid and numerical model by comparing the local Nusselt number (Nu_x) of current study and Shah's correlation. Moreover, profiles of axial velocity of base fluid for different radial location are illustrated in Fig. 3. It can be seen in $x=0.1$ almost the fully developed flow prevails. Shah's correlation is written as:

$$Nu_x = \begin{cases} 1.302 x_*^{\frac{1}{3}} - 1 & x_* \leq 0.00005 \\ 1.302 x_*^{\frac{1}{3}} - 0.5 & 0.00005 < x_* < 0.001 \\ 4.364 + 8.68(10^3 x_*)^{-0.506} e^{-41x_*} & x_* > 0.001 \end{cases} \quad (29)$$

where

$$x_* = \frac{x/D}{Re.Pr} \quad (30)$$

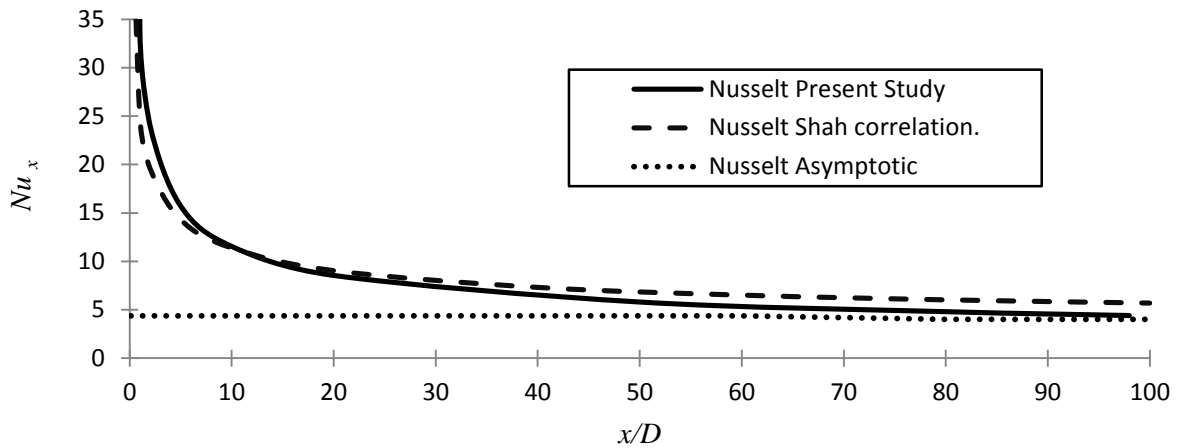


Fig. 2. Comparison of Nusselt number with Shah's correlation.

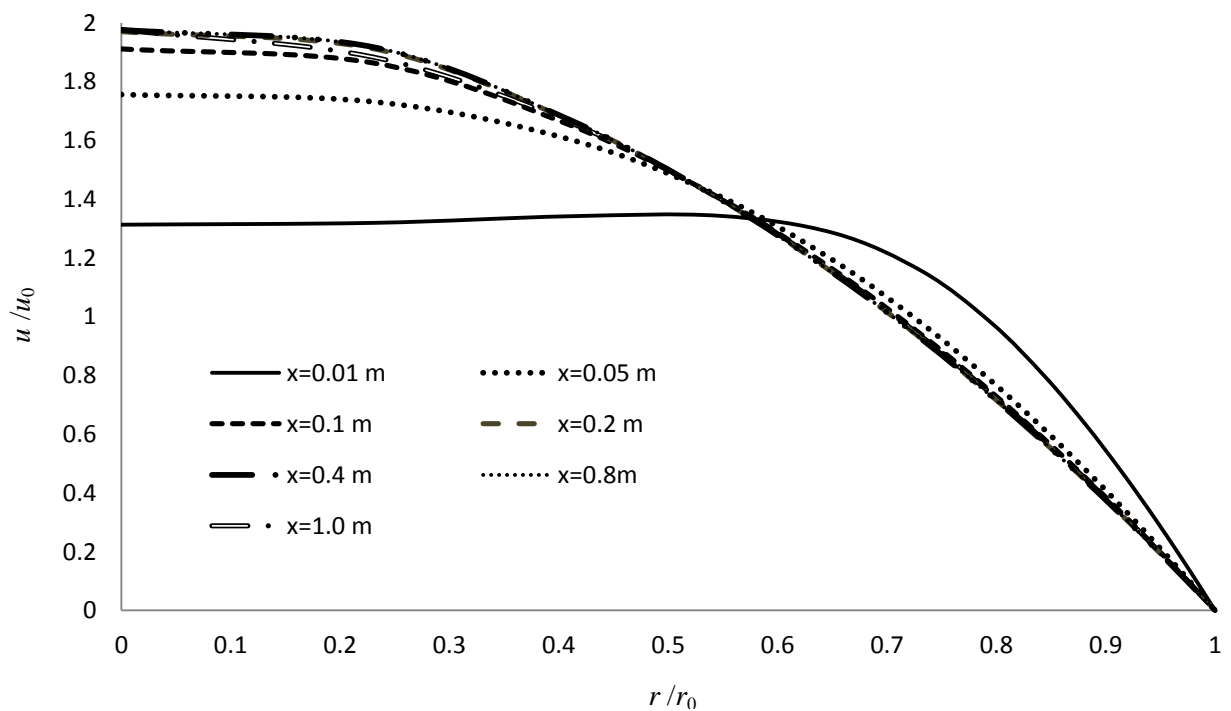


Fig. 3. Axial velocity profiles of base fluid for $Re = 250$.

3. Results and Discussion

Results were obtained by solving discussed governing equations in finite volume method. Single-phase and dispersion models for nanofluid containing Al_2O_3 nanoparticles and water for different particles concentration were employed. Both constant and temperature-dependent properties were taken into account and for all models, size of the particles was considered equal to 20 nm.

Table 2 compares the heat transfer coefficient for base fluid and nanofluid in single-phase and dispersion models for both constant and temperature-dependent thermophysical properties. It can be seen in case of 4% concentration and using the dispersion model in temperature-dependent thermophysical properties, heat transfer coefficient enhances up to 49 %. Also, in all cases, dispersion model with temperature-dependent properties showed higher amount of heat transfer coefficient compared to single-phase model with constant thermophysical properties.

Figure 4 shows the dependency of Nusselt number on Reynolds number at a specific position ($x/D=63$) for 1% concentration of nanoparticles and compares the results to experimental data and a theoretical correlation. By increasing the Reynolds number, Nusselt number for all models improves to a considerable extent. For $Re=750$, dispersion model in temperature-dependent thermophysical properties showed desirable agreements with experimental data of Wen and Ding [2]. Similarly, dispersion model with constant thermophysical properties for $Re=1050$ almost matched with Shah's correlation.

Table 2. Comparison of the heat transfer coefficient for different models for $Re=500$.

Model	Concentration	Type of properties	h_{av}	h_{nf}/h_{bf}
host fluid	0%	constant	333	1
	0%	temperature-dependent	355	1
single-phase	1%	constant	356	1.069
	1%	temperature-dependent	372	1.047
dispersion	1%	constant	371	1.114
	1%	temperature-dependent	387	1.09
single-phase	4%	constant	417	1.252
	4%	temperature-dependent	438	1.233
dispersion	4%	constant	481	1.444
	4%	temperature-dependent	528	1.487

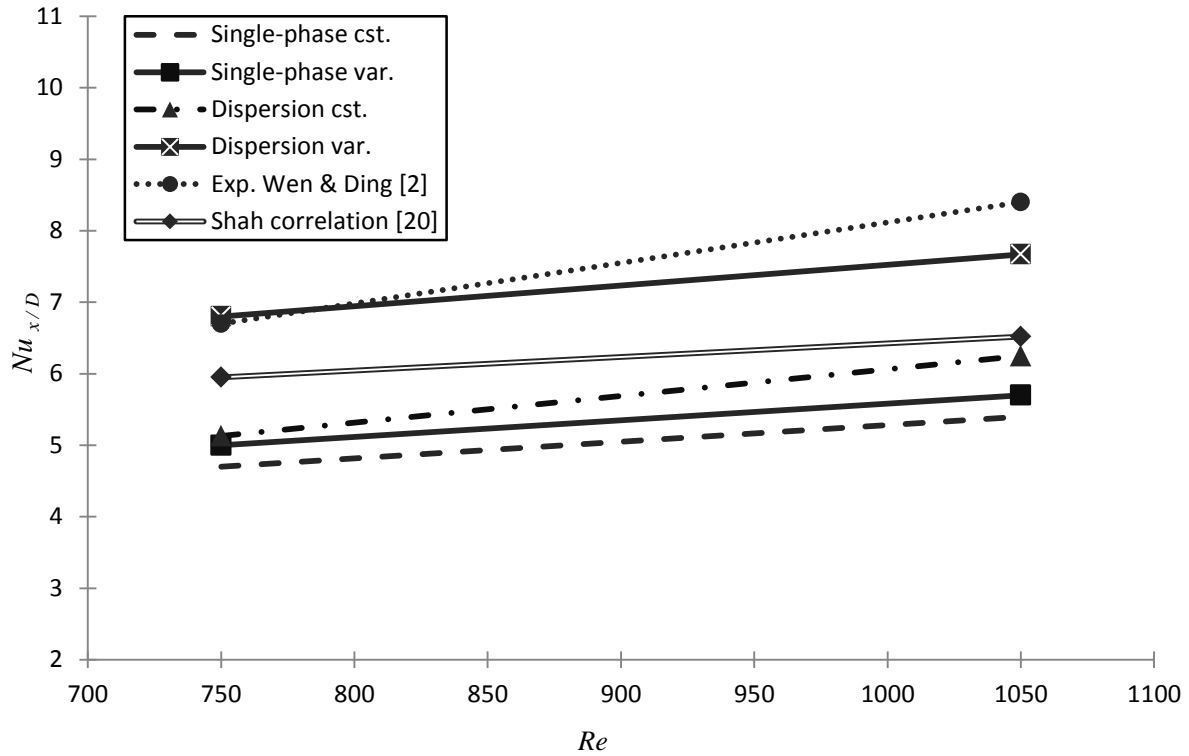


Fig. 4. Dependency of Nusselt number on Reynolds number for $\phi = 0.01$ at $x/D=63$

Figures 5 and 6 illustrate average Nusselt number for different Reynolds numbers for $\phi = 0.01$ and $\phi = 0.04$, respectively. In order to validate the numerical results, various theoretical correlations and experimental data were compared. It can be seen in both figures, dispersion model shows higher values of Nusselt number compared to single-phase model. Moreover, constant properties model in both dispersion and single-phase underestimates the Nusselt number, compared to temperature-dependent properties. Also, it should be noted as Reynolds number and particle concentrations increase, discrepancy between the different models results slightly grows, too. For $\phi = 0.01$, dispersion model in both type of thermophysical properties, and single-phase model only in temperature-dependent thermophysical properties showed a satisfying compatibility with other literatures results. Since Heris et al. [6] conducted their study in constant temperature boundary conditions, for obtaining a precise comparison, results in constant wall heat flux boundary condition is needed. By deriving this fact that Nusselt number in laminar developing flow inside a tube under constant wall heat flux boundary condition is higher than that of under constant wall temperature boundary condition, their results were corrected by means of 20% increase [7, 20].

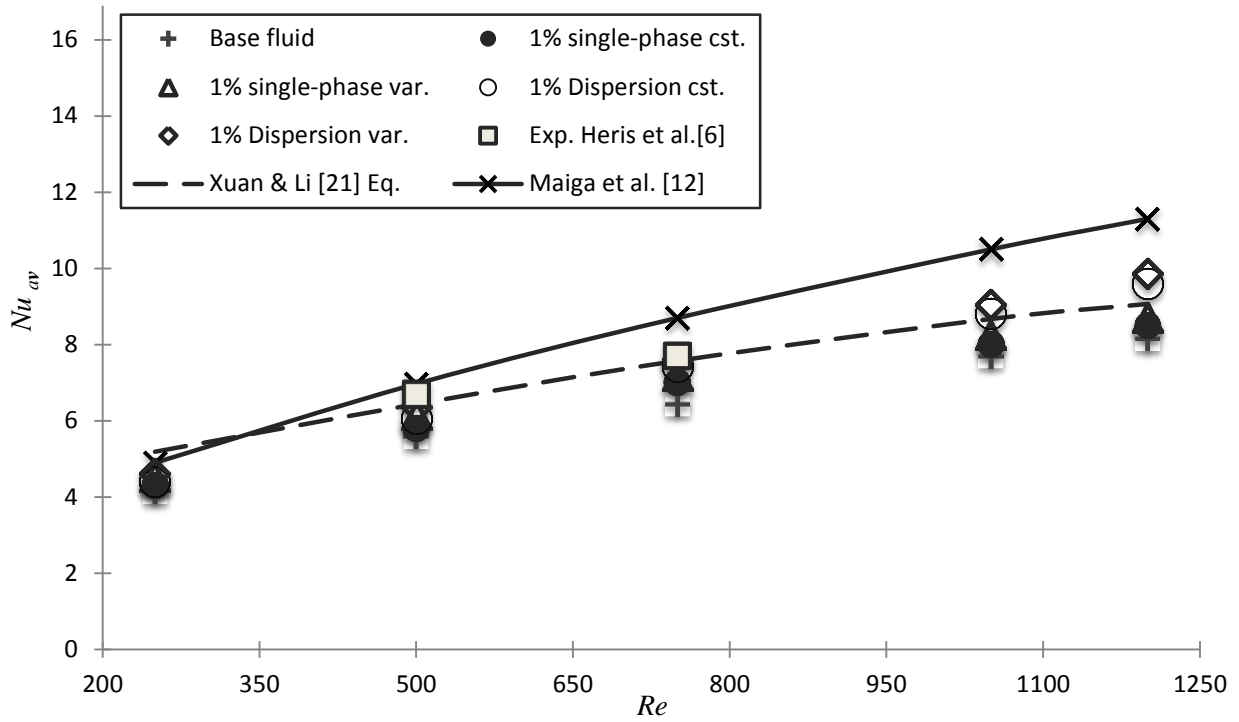


Fig. 5. Average Nusselt number in various Reynolds numbers ($\phi = 0.01$).

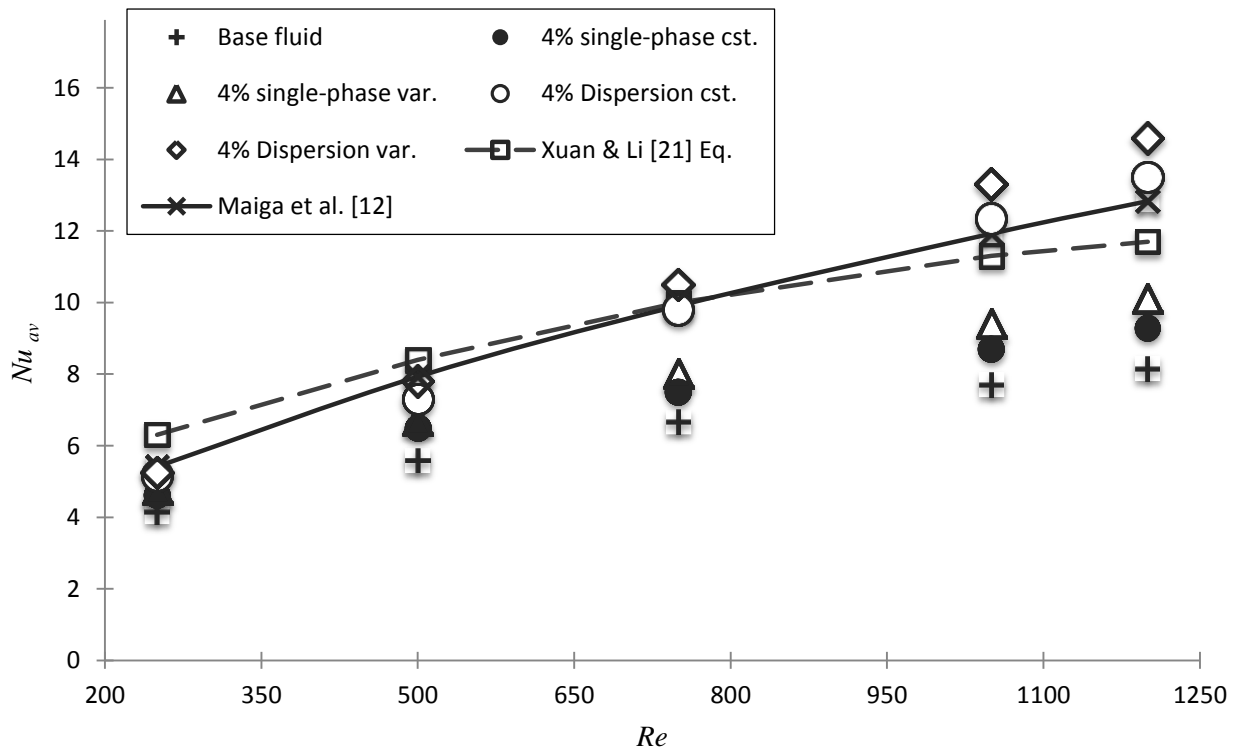


Fig. 6. Average Nusselt number in various Reynolds numbers ($\phi = 0.04$).

In Fig. 6, for $\phi = 0.04$, there is an appropriate agreement between Maiga, et. al. [12], Xuan & Li [21] data and dispersion model in both constant and temperature-dependent thermophysical properties. However, for higher Reynolds numbers it seems temperature-dependent properties model overestimates the Nusselt number. On the other hand, single-phase model in both constant and temperature-dependent properties did not show a desirable compatibility. It can be observed, in cases of lower particle concentration, single-phase model with temperature-dependent thermophysical properties can be satisfying.

Effect of nanoparticle volume concentration on wall temperature of the tube is shown in Fig. 7. By increasing the particles concentration wall temperature decreases and heat transfer coefficient increases. Because for constant wall heat flux boundary condition, decreasing the term of $(T_w - T)$ results in enhancing the heat transfer coefficient and Nusselt number. Also, it can be seen by increasing the particles concentrations, rate of thermal enhancement decreases.

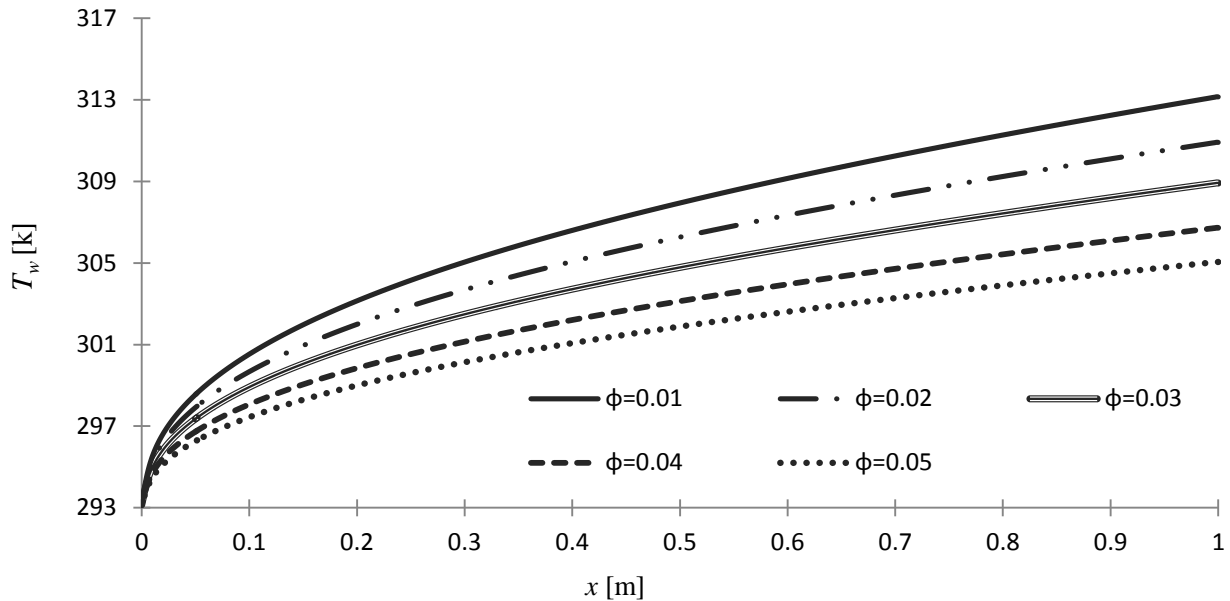


Fig. 7. Effect of nanoparticle concentration on wall temperature for $Re=750$.

Results reported in Table 3 Indicate that shear stress at wall strongly depends on fluid viscosity. By comparing the results it is obvious that average shear stress of temperature-dependent properties are much lower than constant thermophysical properties. This feature is due to this fact that viscosity decreases with temperature. In fact, increasing the average shear stress at wall considered as an undesirable effect. Therefore, showing lower values for shear stress in temperature-dependent model compared to constant properties model, can be an advantage. Since differences between the results of single-phase model and dispersion model were scant (10^{-4} order), only dispersion model results were reported.

Table 3. Comparison of the shear stress values at wall for $Re=750$ in dispersion model.

Model	Concentration	Properties	τ_{av}	τ_{nf}/τ_{bf}
host fluid	0%	constant	0.065	1
	0%	temperature-dependent	0.013	1
dispersion	1%	constant	0.091	1.40
	1%	temperature-dependent	0.017	1.33
dispersion	4%	constant	0.160	2.44
	4%	temperature-dependent	0.033	2.56

4. Conclusion

In this study thermal behavior and wall characteristics of Al_2O_3 - water nanofluid inside a miniature tube were numerically investigated by employing 4 different models: single-phase and dispersion models in both constant and temperature-dependent thermophysical properties.

Results showed that in presence of nanoparticles, heat transfer coefficient and Nusselt number enhance to a large extent. Heat transfer coefficient in case of dispersion model and temperature-dependent properties for $\varphi = 0.04$ showed almost 49% enhancements, while wall shear stress increased more than 2.5 times which can be called as a limitation. However, it can be negligible for lower particle concentrations. Moreover, it was observed Nusselt number strongly depends on Reynolds number and this dependency was much more remarkable in higher particle volume concentration. For each investigated models, dispersion model showed a desirable compatibility with other experimental data and theoretical correlations. The reason behind can be the nature of dispersion model which takes into account irregular and random movements of nanoparticles resulting to boost energy exchange rate. On the other hand, single-phase model underestimated Nusselt number compared to other data, specifically for higher volume concentrations in constant thermophysical properties. Temperature-dependent models compared to constant properties models, showed higher values for Nusselt number which is due to the minimized difference between bulk fluid and wall temperatures.

By considering the effect of viscosity on shear stress, it is obvious that temperature-dependent properties models show lower values for this undesirable term at wall in comparison with constant thermophysical properties in both dispersion and single-phase models. Furthermore, it could be observed at wall, by increasing the particles volume concentration, not only wall temperature decreased, also rate of thermal enhancement decreased slightly.

References

- [1] S. K. Das, S. U. S. Choi, W. Yu, and T. Pradeep, *Nanofluids Science and Technology*. Hoboken, NJ: John Wiley & Sons, 2008.
- [2] D. Wen and Y. Ding, "Experimental investigation into convective heat transfer of nanofluids at the entrance region under laminar flow conditions," *International Journal of Heat and Mass Transfer*, vol. 47, no. 24, pp. 5181–5188, 2004.
- [3] S. Z. Heris, M. N. Esfahany, and G. Etemad, "Numerical investigation of nanofluid laminar convection heat transfer through a circular tube," *Numerical Heat Transfer, Part A*, vol. 52, no. 11, pp. 1043-1058, 2007.
- [4] S. Z. Heris, A. K. Beydokhty, S. H. Noie Baghban, and S. Rezvan, "A numerical study on convective heat transfer of Al_2O_3 /water, CuO/water and Cu/water nanofluids through square cross-section duct in laminar flow," *Engineering Applications of Computational Fluid Mechanics*, vol. 6, no. 1, pp. 1–14, 2012.
- [5] S. Z. Heris, S. H. Noie Baghban, M. Talaii, and J. Sargolzaei, "Numerical investigation of Al_2O_3 /water nanofluid laminar convective heat transfer through triangular ducts," *Nanoscale Research Letters*, vol. 6, no. 1, pp. 1–10, 2012.
- [6] S. Z. Heris, G. Etemad, and M. N. Esfahany, "Experimental investigation of oxide nanofluids laminar flow convective heat transfer," *Int. Comm. Heat Mass Transfer*, vol. 33, no. 4, pp. 529–535, 2006.
- [7] V. Bianco, F. Chiacchio, O. Manca, and S. Nardini, "Numerical investigation of nanofluids forced convection in circular tubes," *Applied Thermal Engineering*, vol. 29, no. 17, pp. 3632–3642, 2009.
- [8] V. Bianco, F. Chiacchio, O. Manca, and S. Nardini, "Numerical investigation on nanofluids turbulent convection heat transfer inside a circular tube," *International Journal of Thermal Sciences*, vol. 50, no. 3, pp. 341–349, 2011.
- [9] R. Lotfi, Y. Saboohi, and A. M. Rashidi, "Numerical study of forced convective heat transfer of nanofluids: Comparison of different approaches," *International Communications in Heat and Mass Transfer*, vol. 37, no. 1, pp. 74–78, 2010.
- [10] A. H. Jahanbin and K. Javaherdeh, "Numerical investigation of CuO nanoparticles effect on forced convective heat transfer inside a mini-channel: Comparison of different approaches," *Life Science Journal*, vol. 10, no. 8s, pp. 183–189, 2013.
- [11] B. C. Pak and Y. I. Cho, "Hydrodynamic and heat transfer study of dispersed fluids with submicron metallic oxide particles," *Exp. Heat Transfer*, vol. 11, no. 2, pp. 151–170, 1998.

- [12] S. E. B. Maiga, S. J. Palm, C. T. Nguyen, G. Roy, and N. Galanis, "Heat transfer enhancement by using nanofluids in forced convection flows," *International Journal of Heat and Fluid Flow*, vol. 26, no. 4, pp. 530–546, 2005.
- [13] S. J. Palm, G. Roy, and C. T. Nguyen, "Heat transfer enhancement with the use of nanofluids in radial flow cooling systems considering temperature-dependent properties," *Applied Thermal Engineering*, vol. 26, no. 17, pp. 2209–2218.
- [14] N. Putra, W. Roetzel, and S. K. Das, "Natural convection of nanofluids," *Heat and Mass Transfer*, vol. 39, no. 8–9, pp. 775–784, 2003.
- [15] Y. Xuan and W. Roetzel, "Conceptions for heat transfer correlation of nanofluids," *Int. J. Heat Mass Transfer*, vol. 43, no. 19, pp. 3701–3707, 2000.
- [16] G. I. Taylor, "The dispersion of matter in turbulent flow in a pipe," in *Proceedings of the Royal Society of London A: Mathematical, Physical and Engineering Sciences*, 1954, vol. 223, pp. 446–468.
- [17] R. Aris, "On the dispersion of a solute in a fluid flowing through a tube," in *Proceedings of the Royal Society of London A: Mathematical, Physical and Engineering Sciences*, 1956, vol. 235, pp. 67–77.
- [18] A. R. A. Khaled and K. Vafai, "Heat transfer enhancement through control of thermal dispersion effects," *Int. J. Heat Mass Transfer*, vol. 48, no. 11, pp. 2172–2185, 2005.
- [19] S. V. Patankar, *Numerical Heat Transfer and Fluid Flow*. New York: Hemisphere Publishing Corporation, Taylor and Francis Group, 1980.
- [20] A. Bejan and A. D. Kraus, *Heat Transfer Handbook*. John Wiley and Sons, 2003.
- [21] S. Kakac and A. Pramuanjaroenki, "Review of convective heat transfer enhancement with nanofluids," *International Journal of Heat and Mass Transfer*, vol. 52, no. 13, pp. 3187–3196, 2009.